Nonreciprocal Optomechanical Entanglement against Backscattering Losses

Ya-Feng Jiao,[1] Sheng-Dian Zhang,[1] Yan-Lei Zhang,[2,3] Adam Miranowicz,[4] Le-Man Kuang,[1,*] and Hui Jing[1,†]
[1]*Key Laboratory of Low-Dimensional Quantum Structures and Quantum Control of Ministry of Education, Department of Physics and Synergetic Innovation Center for Quantum Effects and Applications, Hunan Normal University, Changsha 410081, China*
[2]*CAS Key Laboratory of Quantum Information, University of Science and Technology of China, Hefei 230026, China*
[3]*CAS Center For Excellence in Quantum Information and Quantum Physics, University of Science and Technology of China, Hefei, Anhui 230026, China*
[4]*Faculty of Physics, Adam Mickiewicz University, 61-614 Poznań, Poland*

(Received 9 June 2020; accepted 1 September 2020; published 2 October 2020)

We propose how to achieve nonreciprocal quantum entanglement of light and motion and reveal its counterintuitive robustness against random losses. We find that by splitting the counterpropagating lights of a spinning resonator via the Sagnac effect, photons and phonons can be entangled strongly in a chosen direction but fully uncorrelated in the other. This makes it possible both to realize quantum nonreciprocity even in the absence of any classical nonreciprocity and also to achieve significant entanglement revival against backscattering losses in practical devices. Our work provides a way to protect and engineer quantum resources by utilizing diverse nonreciprocal devices, for building noise-tolerant quantum processors, realizing chiral networks, and backaction-immune quantum sensors.

DOI: 10.1103/PhysRevLett.125.143605

Nonreciprocal physics has witnessed rapid advances in recent years, with unique applications ranging from backaction-immune signal transfer or processing, chiral networking, and invisible sensing [1]. By breaking the Lorentz reciprocity, one-way flow of classical information, i.e., mean photon numbers, has been realized by using atoms [2,3], solid devices [4–12], and synthetic materials [13–19]. Likewise, quantum optical diode or one-way flow of quantum information can also be achieved. In fact, nonreciprocal control of single photons and their quantum fluctuations have been demonstrated, such as single-photon diodes [20,21] or circulators [22], and one-way photon blockade [23,24], providing key tools for chiral quantum engineering [25–28]. However, up to now, the possibilities of switching a single nonreciprocal device between classical and quantum regimes, as well as protecting quantum entanglement with nonreciprocal devices, have not yet been revealed.

Here we propose how to achieve nonreciprocal quantum entanglement in cavity optomechanics (COM), revealing its unique properties which are otherwise unattainable in conventional devices. COM devices featuring coherent light-motion coupling [29,30] have been widely used for quantum control of massive objects [31–36], particularly COM entanglement [37–45] or COM sensors [46–48]. Very recently, quantum correlations at room temperature were observed even between light and 40 kg mirrors [49]. Here we show that COM entanglement can be manipulated in a highly asymmetric way and the resulting nonreciprocal entanglement has the counterintuitive ability to preserve its optimal quality in a chosen direction against losses. This gives a new way to engineer quantum resources by utilizing diverse nonreciprocal devices, without the need of any topological or dissipative structure. In a broader view, our findings shed new light on the marriage of nonreciprocal physics and quantum technology, which can benefit such a wide range of applications as noise-tolerant quantum processing [50,51], chiral quantum networking [25–28,52], and backaction-immune quantum sensing [53–55].

As shown in Fig. 1, we consider a spinning COM resonator evanescently coupled with a tapered fiber. In a recent experiment [15], nonreciprocal propagation of light with 99.6% isolation was demonstrated by using such a spinning device. The optical paths of counterpropagating lights in the resonator are different due to the rotation, resulting in an irreversible refractive index for the clockwise (CW) and counterclockwise (CCW) modes [15]; i.e., $n_{\circlearrowleft,\circlearrowright} = n[1 \pm nR\Omega(n^{-2} - 1)/c]$, where n is the refractive index of the material, Ω is the angular velocity of the resonator with radius R, and c is the speed of light in the vacuum. Correspondingly, the resonance frequencies of the counterpropagating modes experience an opposite Sagnac-Fizeau shift; i.e., $\omega_c \to \omega_c + \Delta_F$, with [56]

$$\Delta_F = \pm\Omega \frac{nR\omega_c}{c}\left(1 - \frac{1}{n^2} - \frac{\lambda}{n}\frac{dn}{d\lambda}\right), \qquad (1)$$

where ω_c is the resonance frequency for a stationary resonator, and λ is the light wavelength in vacuum. The dispersion term $dn/d\lambda$, characterizing the relativistic origin

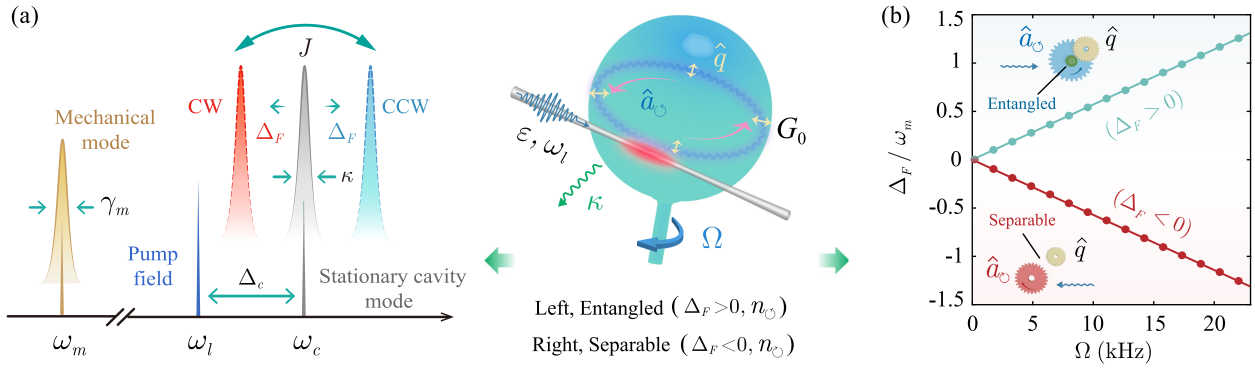

FIG. 1. Nonreciprocal optomechanical entanglement in a spinning resonator. (a) Frequency spectrum of the spinning COM system. By fixing the CW rotation of the resonator, we have $\Delta_F > 0$ ($\Delta_F < 0$) for the case by driving the CCW (CW) mode. Besides, the resonator can support a radiation-pressure-induced mechanical radial breathing mode. The CW and CCW modes are coupled via backscattering with the strength J. (b) The Sagnac-Fizeau shift Δ_F versus the angular velocity Ω. Increasing the angular velocity results in a linear opposite frequency shift for the counterpropagating modes. For the same input light, due to the opposite frequency shift for the counterpropagating modes, COM entanglement can appear unidirectionally. See the text for more details.

of the Sagnac effect, is small in typical materials (up to $\sim$1%) [15,56]. By spinning the resonator along the CW direction, we have $\Delta_F > 0$ or $\Delta_F < 0$ for the case with the driving laser on the left- or right-hand side, and the corresponding effective optical frequencies are $\omega_j \equiv \omega_c \pm |\Delta_F|$ ($j = \circlearrowleft, \circlearrowright$), respectively. In addition, the resonator can support a mechanical breathing mode with frequency ω_m. In a rotating frame with respect to $\hat H_0 = \hbar\omega_l(\hat a^\dagger_\circlearrowleft \hat a_\circlearrowleft + \hat a^\dagger_\circlearrowright \hat a_\circlearrowright)$, the Hamiltonian of this spinning COM system, with the driving laser on the left-hand side, is this:

$$\hat H = \hat{\mathcal{H}}_c + \frac{\hbar\omega_m}{2}(\hat p^2 + \hat q^2) - \hbar G_0(\hat a^\dagger_\circlearrowright \hat a_\circlearrowright + \hat a^\dagger_\circlearrowleft \hat a_\circlearrowleft)\hat q,$$
$$\hat{\mathcal{H}}_c = \sum_{j=\circlearrowleft,\circlearrowright} \hbar\Delta_j \hat a^\dagger_j \hat a_j + \hbar J(\hat a^\dagger_\circlearrowright \hat a_\circlearrowleft + \hat a^\dagger_\circlearrowleft \hat a_\circlearrowright) + i\hbar\varepsilon(\hat a^\dagger_\circlearrowleft - \hat a_\circlearrowleft), \tag{2}$$

where $\hat a_j$ ($\hat a^\dagger_j$) is the optical annihilation (creation) operator, $\Delta_j = \omega_j - \omega_l$, and $\hat q$ ($\hat p$) is the dimensionless mechanical displacement (momentum) operator. The frame rotating with driving frequency ω_l is obtained by applying the unitary transformation $\hat U = \exp[i\hat H_0 t/\hbar]$ (see, e.g., Ref. [29]). The field amplitude of the driving laser is $|\varepsilon| = \sqrt{2\kappa P/\hbar\omega_l}$, where P and κ are the input laser power and the optical decay rate, respectively. $G_0 = (\omega_c/R) \times \sqrt{\hbar/m\omega_m}$ denotes the single-photon COM coupling rate [29], with m the mass of the resonator. Also, imperfections of devices, such as surface roughness or material defect, can cause optical backscattering, as described by the mode-coupling strength J. In a recent experiment, by breaking the time-reversal symmetry with Brillouin devices, dynamical suppression of the backscattering was already observed [57].

Quantum Langevin equations of this spinning COM system then read:

$$\dot{\hat a}_\circlearrowleft = -(i\Delta_\circlearrowleft + \kappa)\hat a_\circlearrowleft - iJ\hat a_\circlearrowright + iG_0\hat a_\circlearrowleft \hat q + \varepsilon + \sqrt{2\kappa}\hat a^{\text{in}}_\circlearrowleft,$$
$$\dot{\hat a}_\circlearrowright = -(i\Delta_\circlearrowright + \kappa)\hat a_\circlearrowright - iJ\hat a_\circlearrowleft + iG_0\hat a_\circlearrowright \hat q + \sqrt{2\kappa}\hat a^{\text{in}}_\circlearrowright,$$
$$\dot{\hat q} = \omega_m \hat p,$$
$$\dot{\hat p} = -\omega_m \hat q - \gamma_m \hat p + G_0(\hat a^\dagger_\circlearrowright \hat a_\circlearrowright + \hat a^\dagger_\circlearrowleft \hat a_\circlearrowleft) + \hat\xi, \tag{3}$$

where γ_m is the mechanical damping rate, and $\hat a^{\text{in}}_j$ ($\hat\xi$) is the zero-mean input noise operator for the optical (mechanical) mode, characterized by the following correlation functions [58]:

$$\langle \hat a^{\text{in}}_j(t)\hat a^{\text{in},\dagger}_j(t')\rangle = \delta(t-t'),$$
$$\langle \hat\xi(t)\hat\xi(t')\rangle \simeq \gamma_m(2n_m+1)\delta(t-t'), \quad \text{for } \omega_m/\gamma_m \gg 1, \tag{4}$$

where $n_m = [\exp(\hbar\omega_m/k_B\mathrm{T}) - 1]^{-1}$ denotes the thermal phonon number, k_B is the Boltzmann constant, and T is the bath temperature. Under the condition of strong optical driving, we can linearize the dynamics by expanding each operator as a sum of its steady-state value and a small fluctuation around it, i.e., $\hat a_j = \alpha_j + \delta\hat a_j$, $\hat q = q_s + \delta\hat q$, $\hat p = p_s + \delta\hat p$. By defining the vectors of quadrature fluctuations and input noises as $u^T(t) = (\delta\hat X_\circlearrowleft, \delta\hat Y_\circlearrowleft, \delta\hat X_\circlearrowright, \delta\hat Y_\circlearrowright, \delta\hat q, \delta\hat p)$, $v^T(t) = (\sqrt{2\kappa}\hat X^{\text{in}}_\circlearrowleft, \sqrt{2\kappa}\hat Y^{\text{in}}_\circlearrowleft, \sqrt{2\kappa}\hat X^{\text{in}}_\circlearrowright, \sqrt{2\kappa}\hat Y^{\text{in}}_\circlearrowright, 0, \hat\xi)$, with the components:

$$\delta\hat X_j = \frac{1}{\sqrt 2}(\delta\hat a^\dagger_j + \delta\hat a_j), \qquad \delta\hat Y_j = \frac{i}{\sqrt 2}(\delta\hat a^\dagger_j - \delta\hat a_j),$$
$$\hat X^{\text{in}}_j = \frac{1}{\sqrt 2}(\hat a^{\text{in}\dagger}_j + \hat a^{\text{in}}_j), \qquad \hat Y^{\text{in}}_j = \frac{i}{\sqrt 2}(\hat a^{\text{in}\dagger}_j - \hat a^{\text{in}}_j), \tag{5}$$

we obtain a compact form of the linearized equations of quantum fluctuations: $\dot{u}(t) = Au(t) + v(t)$, where

$$A = \begin{pmatrix} -\kappa & \tilde{\Delta}_{\circlearrowleft} & 0 & J & -G^y_{\circlearrowleft} & 0 \\ -\tilde{\Delta}_{\circlearrowleft} & -\kappa & -J & 0 & G^x_{\circlearrowleft} & 0 \\ 0 & J & -\kappa & \tilde{\Delta}_{\circlearrowright} & -G^y_{\circlearrowright} & 0 \\ -J & 0 & -\tilde{\Delta}_{\circlearrowright} & -\kappa & G^x_{\circlearrowright} & 0 \\ 0 & 0 & 0 & 0 & 0 & \omega_m \\ G^x_{\circlearrowleft} & G^y_{\circlearrowleft} & G^x_{\circlearrowright} & G^y_{\circlearrowright} & -\omega_m & -\gamma_m \end{pmatrix}, \quad (6)$$

and $\tilde{\Delta}_j = \Delta_j - G_0 q_s$ is the effective optical detuning, G^x_j (G^y_j) is the real (imaginary) part of the effective COM coupling rate $(G_j \equiv \sqrt{2}G_0\alpha_j = G^x_j + iG^y_j)$, and the steady-state mean values of the dynamical variables are given by

$$\alpha_{\circlearrowleft} = \frac{(i\tilde{\Delta}_{\circlearrowright} + \kappa)\varepsilon}{(i\tilde{\Delta}_{\circlearrowright} + \kappa)(i\tilde{\Delta}_{\circlearrowleft} + \kappa) + J^2},$$
$$\alpha_{\circlearrowright} = \frac{-iJ}{(i\tilde{\Delta}_{\circlearrowright} + \kappa)}\alpha_{\circlearrowleft},$$
$$q_s = \frac{G_0}{\omega_m}(|\alpha_{\circlearrowright}|^2 + |\alpha_{\circlearrowleft}|^2),$$
$$p_s = 0. \quad (7)$$

The solution of the linearized Langevin equations is given by $u(t) = \mathcal{M}(t)u(0) + \int_0^t d\tau \mathcal{M}(\tau)v(t-\tau)$, where $\mathcal{M}(t) = \exp(At)$. The system is stable and reaches its steady state when all real parts of the eigenvalues of A are negative, as characterized by the Routh-Hurwitz criterion [59,60]. When the stability condition is fulfilled, we have $\mathcal{M}(\infty) = 0$ in the steady state and

$$u_i(\infty) = \int_0^\infty d\tau \sum_k \mathcal{M}_{ik}(\tau)v_k(t-\tau). \quad (8)$$

Due to the linearized dynamics and the Gaussian nature of the quantum noises, the steady state of the system, independently of any initial conditions, finally evolves into a tripartite zero-mean Gaussian state, which is fully characterized by a 6×6 correlation matrix V, with its components

$$V_{kl} = \langle u_k(\infty)u_l(\infty) + u_l(\infty)u_k(\infty)\rangle/2. \quad (9)$$

By substituting Eq. (8) into Eq. (9) and using the fact that the six components of $v(t)$ are uncorrelated, the steady-state correlation matrix V is obtained as

$$V = \int_0^\infty d\tau \mathcal{M}(\tau) D \mathcal{M}^T(\tau), \quad (10)$$

where $D = \mathrm{Diag}[\kappa, \kappa, \kappa, \kappa, 0, \gamma_m(2n_m + 1)]$ is the diffusion matrix, defined through $\langle v_k(\tau)v_l(\tau') + v_l(\tau')v_k(\tau)\rangle/2 = D_{kl}\delta(\tau - \tau')$. Under the stability condition, the steady-state correlation matrix V fulfills the Lyapunov equation [37]:

$$AV + VA^T = -D. \quad (11)$$

This linear Eq. (11) allows us to find V for any values of the relevant parameters. To quantify the entanglement between the mechanical mode and the driven optical mode, we adopt

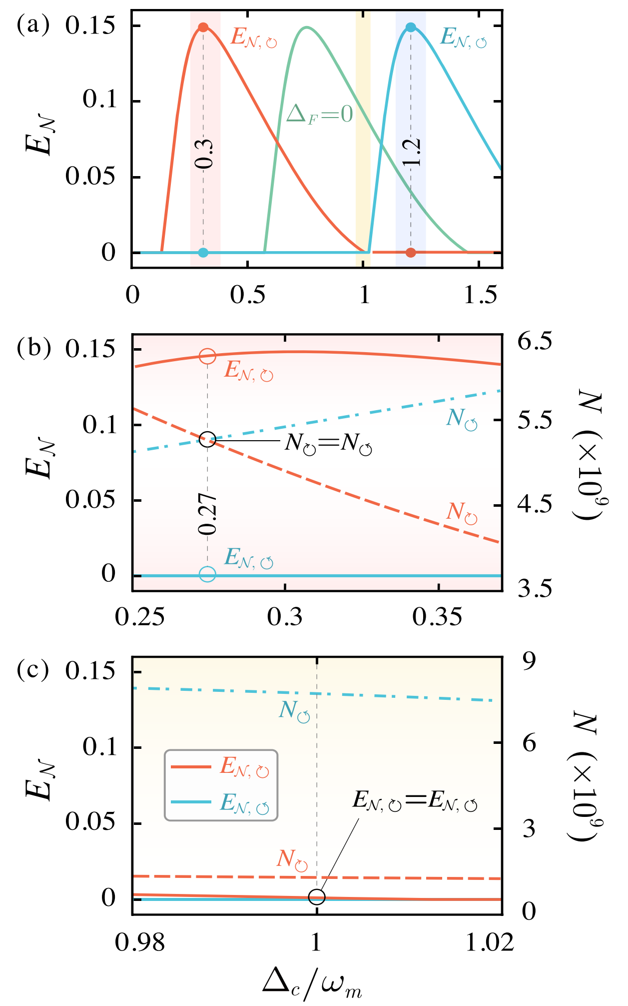

FIG. 2. Nonreciprocal COM entanglement without backscattering. (a) $E_{\mathcal{N}}$ versus Δ_c/ω_m for different input directions. For $\Delta_F = 0$, COM entanglement exists around the resonance $\Delta_c/\omega_m \simeq 1$. The spectral offset is due to the COM-induced redshift of the cavity mode. For $\Delta_F \neq 0$, the resonance conditions for the countercirculating modes are modified by the opposite Sagnac shifts, resulting in the peaks symmetrically shifted for the opposite input directions. (b)–(c) Tunable quantum nonreciprocity versus classical nonreciprocity. For $\Delta_c/\omega_m \sim 0.27$, quantum nonreciprocity exists even when $N_{\circlearrowleft} = N_{\circlearrowright}$ (without classical nonreciprocity); in contrast, for $\Delta_c/\omega_m \sim 1$, classical nonreciprocity appears for $E_{\mathcal{N},\circlearrowleft} = E_{\mathcal{N},\circlearrowright}$. The parameters are chosen as $\Omega = 8$ kHz, $J = 0$, and $P = 20$ mW.

the logarithmic negativity, $E_\mathcal{N}$, as a bipartite entanglement measure for continuous variables [68]

$$E_\mathcal{N} = \max[0, -\ln(2\nu^-)], \tag{12}$$

where $\nu^- = 2^{-1/2}\{\Sigma(V') - [\Sigma(V')^2 - 4\det V']^{1/2}\}^{1/2}$, with $\Sigma(V') = \det\mathcal{A} + \det\mathcal{B} - 2\det\mathcal{C}$, is the smallest eigenvalue of the partial transpose of the reduced correlation matrix V'. By tracing out the reflected mode in V and writing it in a 2×2 block form, we have

$$V' = \begin{pmatrix} \mathcal{A} & \mathcal{C} \\ \mathcal{C}^T & \mathcal{B} \end{pmatrix}. \tag{13}$$

V' preserves the Gaussian nature, and entanglement emerges in its corresponding subsystem if and only if $\nu^- < 1/2$, which is equivalent to Simon's necessary and sufficient entanglement criterion (or the related Peres-Horodecki criterion) for certifying entanglement of two-mode system in Gaussian states [69].

In our calculations, for ensuring the stability of the system, we use the experimentally feasible values [15,70]: $n = 1.48$, $m = 10$ ng, $R = 1.1$ mm, $\lambda = 1.55$ μm, $Q = \omega_c/\kappa = 3.2\times 10^7$, $\omega_m = 63$ MHz, $\gamma_m = 5.2$ kHz, T = 130 mK, and $\Omega = 8$ kHz or 23 kHz. We first consider the case without backscattering, i.e., $J = 0$. In Fig. 2, we plot the logarithmic negativity $E_{\mathcal{N},j}$ and the intracavity photon number $N_j \equiv |\alpha_j|^2$ of the driven mode, as a function of the detuning $\Delta_c = \omega_c - \omega_l$. Here j denotes the driving direction. For a stationary resonator, $E_{\mathcal{N},j}$ is independent on the driving direction, while for a spinning one, it becomes different by reversing the direction. For example, Figs. 2(a) and 2(b) show that, when the maximal COM entanglement is created by driving from one side, no entanglement occurs by driving it from the other side. The underlying physics can be understood as follows. In COM, the driving laser is scattered by the mechanical mode into the Stokes and anti-Stokes sidebands. When the cavity mode is resonant with one of the sidebands, COM correlations are created, as shown in experiments [40,41]. Now, by spinning the resonator, nonreciprocity emerges for the created COM entanglement, which is fundamentally different from classical nonreciprocity of mean photon numbers. In fact, as shown in Figs. 2(b) and 2(c), nonreciprocal COM entanglement exists even without any classical nonreciprocity; in contrast, for $\Delta_c/\omega_m \sim 1$, significant classical nonreciprocity appears for $E_{\mathcal{N},\circlearrowleft} \simeq E_{\mathcal{N},\circlearrowright}$. Hence it is possible to switch a single nonreciprocal device between classical and quantum regimes. We note that one-way quantum control of photon

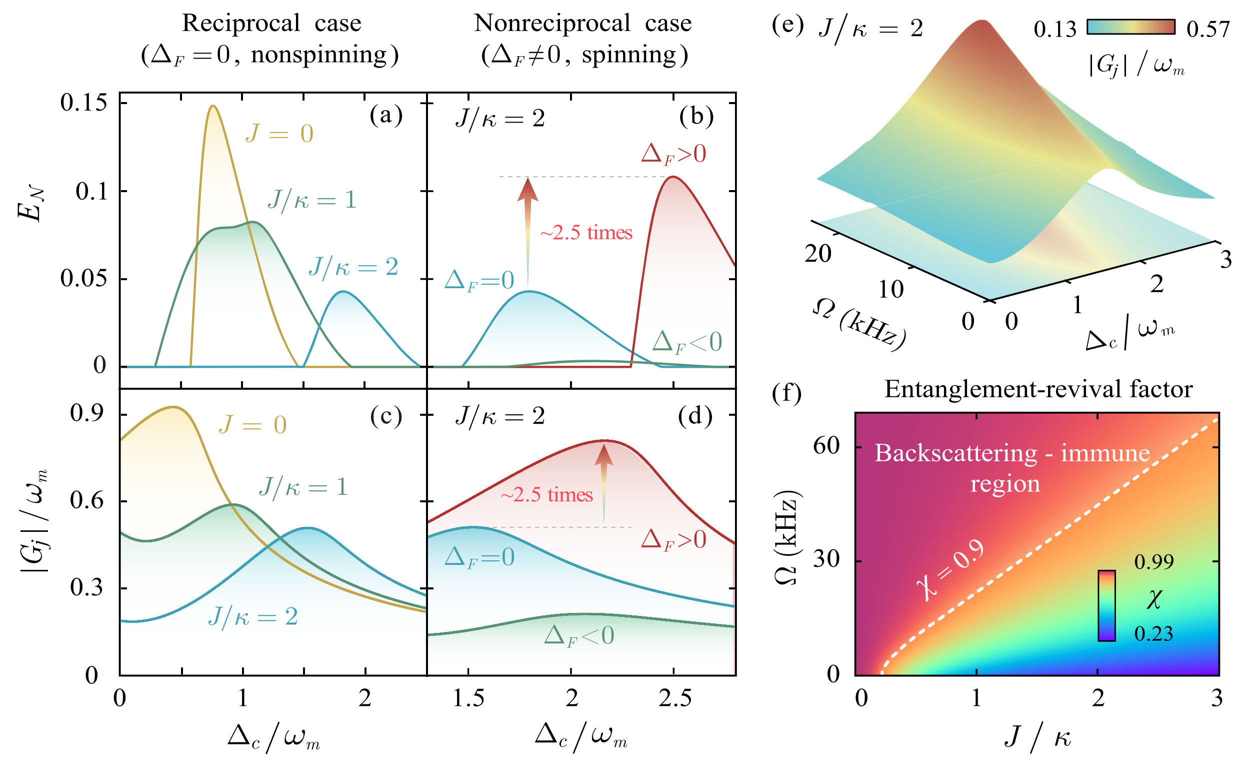

FIG. 3. Suppression of COM entanglement due to random-defect-induced backscattering, and its nonreciprocal revival resulting from the rotation-induced compensation. (a),(b) The logarithmic negativity $E_\mathcal{N}$ and (c),(d) the effective COM coupling $|G_j|/\omega_m$ are plotted as a function of the scaled optical detuning Δ_c/ω_m. For $\Omega = 23$ kHz, the value of $E_\mathcal{N}$ is enhanced for ~2.5 times, reaching almost that as in an ideal device without backscattering. (e) The effective COM coupling $|G_j|/\omega_m$ versus the optical detuning Δ_c/ω_m and the rotation speed Ω. (f) Density plot of the revival factor χ as a function of the optical coupling strength J and the rotation speed Ω.

bunching and antibunching has been observed very recently [22,24].

More importantly, quantum nonreciprocity provides a feasible way to protect devices against losses, which is reminiscent of that in topological systems or chiral environment [26,27]. Figure 3(a) shows that, in conventional COM, $E_{\mathcal{N}}$ decreases for $J \neq 0$, while for a spinning device, the maximum value of $E_{\mathcal{N}}$ is significantly enhanced, approaching to that in an ideal device [see Fig. 3(b)]. To better understand this counterintuitive effect, we also plot the effective COM coupling of the driven mode $|G_j|$ with respect to Δ_c in Figs. 3(c)–3(e). We see that the backscattering-induced reflection can be significantly suppressed in a spinning device. As a result, one can achieve nearly ideal COM entanglement, which can be clearly shown by defining a revival factor:

$$\chi = \frac{\max\left[E_{\mathcal{N}}(\Omega \neq 0, J \neq 0)\right]}{\max\left[E_{\mathcal{N}}(\Omega = 0, J = 0)\right]}. \tag{14}$$

Figure 3(f) shows that the maximal factor can reach 99.1%; i.e., COM entanglement in such a nonreciprocal device is immune to random losses. This provides a new strategy to improve the performance of quantum devices by harnessing the power of nonreciprocity. Also we have confirmed that nonreciprocal entanglement can survive even when quantum COM entanglement is fully destroyed by thermal noises in a conventional reciprocal device (see the Supplemental Material for more details [60]).

Finally, we remark that in experiments, COM entanglement can be detected by measuring the correlation matrix V under a proper readout choice via a filter [39–41]. The optical quadratures can be measured via a homodyne or heterodyne detection of the output [41–43], and the readout of mechanical ones requires a probe being resonant with the anti-Stokes sideband, mapping the mechanical motion to the output field [41,44]. With the same procedure, nonreciprocal features are observable also in the output field, including transmission rates [71] and COM correlations [40–45], detailed calculations of which will be given elsewhere.

In summary, we have shown how to achieve quantum nonreciprocal entanglement in a COM system, how to switch such a single nonreciprocal device between classical and quantum regimes, and how to keep the optimal entanglement in a chosen direction against losses. These findings, shedding light on the marriage of nonreciprocal physics and quantum engineering, open up the way to control quantum states by utilizing such diverse nonreciprocal devices as in optics, atomtronics [21,22,24], electronics [72], and in acoustics [73]. In fact, quantum nonreciprocity is achievable in systems well beyond COM; for instance, one-way control of sub- or super-Poissonian correlations, as predicted in an optical system [23], was demonstrated very recently using cavity atoms [24]. In a broader view, nonreciprocal entanglement provides an unconventional tool for tasks that cannot be performed by classical one-way devices, such as building noise-tolerant quantum processors [50] and achieving directional quantum sensing [33–36] or steering multipartite entanglement [74–77].

We thank Chang-Ling Zou and Ran Huang for discussions. A. M. is supported by the Polish National Science Centre under the Maestro Grant No. DEC-2019/34/A/ST2/00081. L.-M. K. is supported by the National Natural Science Foundation of China (NSFC, Grants No. 11775075 and No. 11434011), and H. J. is supported by the NSFC (Grants No. 11774086 and No. 11935006). Y.-L. Z. is supported by the NSFC (Grants No. 11704370) and the China Postdoctoral Science Foundation (2019M652181).

*lmkuang@hunnu.edu.cn
†jinghui73@gmail.com

[1] Y. Shoji and T. Mizumoto, Magneto-optical non-reciprocal devices in silicon photonics, Sci. Technol. Adv. Mater. **15**, 014602 (2014).

[2] H. Ramezani, P. K. Jha, Y. Wang, and X. Zhang, Nonreciprocal Localization of Photons, Phys. Rev. Lett. **120**, 043901 (2018).

[3] S. Zhang, Y. Hu, G. Lin, Y. Niu, K. Xia, J. Gong, and S. Gong, Thermal-motion-induced non-reciprocal quantum optical system, Nat. Photonics **12**, 744 (2018).

[4] C.-H. Dong, Z. Shen, C.-L. Zou, Y.-L. Zhang, W. Fu, and G.-C. Guo, Brillouin-scattering-induced transparency and non-reciprocal light storage, Nat. Commun. **6**, 6193 (2015).

[5] J. Kim, M. C. Kuzyk, K. Han, H. Wang, and G. Bahl, Non-reciprocal Brillouin scattering induced transparency, Nat. Phys. **11**, 275 (2015).

[6] X.-W. Xu, Y. Li, B. Li, H. Jing, and A.-X. Chen, Nonreciprocity via Nonlinearity and Synthetic Magnetism, Phys. Rev. Applied **13**, 044070 (2020).

[7] S. Manipatruni, J. T. Robinson, and M. Lipson, Optical Nonreciprocity in Optomechanical Structures, Phys. Rev. Lett. **102**, 213903 (2009).

[8] Z. Shen, Y.-L. Zhang, Y. Chen, C.-L. Zou, Y.-F. Xiao, X.-B. Zou, F.-W. Sun, G.-C. Guo, and C.-H. Dong, Experimental realization of optomechanically induced non-reciprocity, Nat. Photonics **10**, 657 (2016).

[9] N. R. Bernier, L. D. Tóth, A. Koottandavida, M. A. Ioannou, D. Malz, A. Nunnenkamp, A. K. Feofanov, and T. J. Kippenberg, Nonreciprocal reconfigurable microwave optomechanical circuit, Nat. Commun. **8**, 604 (2017).

[10] L. Mercier de Lépinay, E. Damskägg, C. F. Ockeloen-Korppi, and M. A. Sillanpää, Realization of Directional Amplification in a Microwave Optomechanical Device, Phys. Rev. Applied **11**, 034027 (2019).

[11] K. Fang, J. Luo, A. Metelmann, M. H. Matheny, F. Marquardt, A. A. Clerk, and O. Painter, Generalized nonreciprocity in an optomechanical circuit via synthetic magnetism and reservoir engineering, Nat. Phys. **13**, 465 (2017).

[12] M. Hafezi and P. Rabl, Optomechanically induced non-reciprocity in microring resonators, Opt. Express **20**, 7672 (2012).
[13] D.-W. Wang, H.-T. Zhou, M.-J. Guo, J.-X. Zhang, J. Evers, and S.-Y. Zhu, Optical Diode Made from a Moving Photonic Crystal, Phys. Rev. Lett. **110**, 093901 (2013).
[14] Y. Yang, C. Peng, D. Zhu, H. Buljan, J. D. Joannopoulos, B. Zhen, and M. Soljačić, Synthesis and observation of non-Abelian gauge fields in real space, Science **365**, 1021 (2019).
[15] S. Maayani, R. Dahan, Y. Kligerman, E. Moses, A. U. Hassan, H. Jing, F. Nori, D. N. Christodoulides, and T. Carmon, Flying couplers above spinning resonators generate irreversible refraction, Nature (London) **558**, 569 (2018).
[16] D. L. Sounas and A. Alù, Non-reciprocal photonics based on time modulation, Nat. Photonics **11**, 774 (2017).
[17] B. Peng, Ş. K. Özdemir, F. Lei, F. Monifi, M. Gianfreda, G. L. Long, S. Fan, F. Nori, C. M. Bender, and L. Yang, Parity-time-symmetric whispering-gallery microcavities, Nat. Phys. **10**, 394 (2014).
[18] B. Peng, Ş. K. Özdemir, M. Liertzer, W. Chen, J. Kramer, H. Yilmaz, J. Wiersig, S. Rotter, and L. Yang, Chiral modes and directional lasing at exceptional points, Proc. Natl. Acad. Sci. U.S.A. **113**, 6845 (2016).
[19] Q. Zhong, S. Nelson, Ş. K. Özdemir, and R. El-Ganainy, Controlling directional absorption with chiral exceptional surfaces, Opt. Lett. **44**, 5242 (2019).
[20] K. Xia, F. Nori, and M. Xiao, Cavity-Free Optical Isolators and Circulators Using a Chiral Cross-Kerr Nonlinearity, Phys. Rev. Lett. **121**, 203602 (2018).
[21] M.-X. Dong, Y.-C. Yu, Y.-H. Ye *et al.*, Experimental realization of quantum non-reciprocity based on cold atomic ensembles, arXiv:1908.09242.
[22] M. Scheucher, A. Hilico, E. Will, J. Volz, and A. Rauschenbeutel, Quantum optical circulator controlled by a single chirally coupled atom, Science **354**, 1577 (2016).
[23] R. Huang, A. Miranowicz, J.-Q. Liao, F. Nori, and H. Jing, Nonreciprocal Photon Blockade, Phys. Rev. Lett. **121**, 153601 (2018).
[24] P. Yang, M. Li, X. Han, H. He, G. Li, C.-L. Zou, P. Zhang, and T. Zhang, Non-reciprocal cavity polariton, arXiv:1911.10300.
[25] P. Lodahl, S. Mahmoodian, S. Stobbe, A. Rauschenbeutel, P. Schneeweiss, J. Volz, H. Pichler, and P. Zoller, Chiral quantum optics, Nature (London) **541**, 473 (2017).
[26] C. Gonzalez-Ballestero, A. Gonzalez-Tudela, F. J. Garcia-Vidal, and E. Moreno, Chiral route to spontaneous entanglement generation, Phys. Rev. B **92**, 155304 (2015).
[27] S. A. H. Gangaraj, G. W. Hanson, and M. Antezza, Robust entanglement with three-dimensional nonreciprocal photonic topological insulators, Phys. Rev. A **95**, 063807 (2017).
[28] G. Hu, X. Hong, K. Wang *et al.*, Coherent steering of nonlinear chiral valley photons with a synthetic Au-WS_2 metasurface, Nat. Photonics **13**, 467 (2019).
[29] M. Aspelmeyer, T. J. Kippenberg, and F. Marquardt, Cavity optomechanics, Rev. Mod. Phys. **86**, 1391 (2014).
[30] E. Verhagen, S. Deléglise, S. Weis, A. Schliesser, and T. J. Kippenberg, Quantum-coherent coupling of a mechanical oscillator to an optical cavity mode, Nature (London) **482**, 63 (2012).
[31] S. Hong, R. Riedinger, I. Marinković, A. Wallucks, S. G. Hofer, R. A. Norte, M. Aspelmeyer, and S. Gröblacher, Hanbury Brown and Twiss interferometry of single phonons from an optomechanical resonator, Science **358**, 203 (2017).
[32] F. Lecocq, J. B. Clark, R. W. Simmonds, J. Aumentado, and J. D. Teufel, Quantum Nondemolition Measurement of a Nonclassical State of a Massive Object, Phys. Rev. X **5**, 041037 (2015).
[33] E. E. Wollman, C. U. Lei, A. J. Weinstein, J. Suh, A. Kronwald, F. Marquardt, A. A. Clerk, and K. C. Schwab, Quantum squeezing of motion in a mechanical resonator, Science **349**, 952 (2015).
[34] J.-M. Pirkkalainen, E. Damskägg, M. Brandt, F. Massel, and M. A. Sillanpää, Squeezing of Quantum Noise of Motion in a Micromechanical Resonator, Phys. Rev. Lett. **115**, 243601 (2015).
[35] K. Stannigel, P. Rabl, A. S. Sørensen, P. Zoller, and M. D. Lukin, Optomechanical Transducers for Long-Distance Quantum Communication, Phys. Rev. Lett. **105**, 220501 (2010).
[36] M. Mirhosseini, A. Sipahigil, M. Kalaee, and O. Painter, Quantum transduction of optical photons from a superconducting qubit, arXiv:2004.04838.
[37] D. Vitali, S. Gigan, A. Ferreira, H. R. Böhm, P. Tombesi, A. Guerreiro, V. Vedral, A. Zeilinger, and M. Aspelmeyer, Optomechanical Entanglement Between a Movable Mirror and a Cavity Field, Phys. Rev. Lett. **98**, 030405 (2007).
[38] S. Huang and G. S. Agarwal, Entangling nanomechanical oscillators in a ring cavity by feeding squeezed light, New J. Phys. **11**, 103044 (2009).
[39] C. Genes, A. Mari, P. Tombesi, and D. Vitali, Robust entanglement of a micromechanical resonator with output optical fields, Phys. Rev. A **78**, 032316 (2008).
[40] R. Riedinger, S. Hong, R. A. Norte, J. A. Slater, J. Shang, A. G. Krause, V. Anant, M. Aspelmeyer, and S. Gröblacher, Non-classical correlations between single photons and phonons from a mechanical oscillator, Nature (London) **530**, 313 (2016).
[41] T. A. Palomaki, J. D. Teufel, R. W. Simmonds, and K. W. Lehnert, Entangling mechanical motion with microwave fields, Science **342**, 710 (2013).
[42] S. Barzanjeh, E. S. Redchenko, M. Peruzzo, M. Wulf, D. P. Lewis, G. Arnold, and J. M. Fink, Stationary entangled radiation from micromechanical motion, Nature (London) **570**, 480 (2019).
[43] J. Chen, M. Rossi, D. Mason, and A. Schliesser, Entanglement of propagating optical modes via a mechanical interface, Nat. Commun. **11**, 943 (2020).
[44] C. F. Ockeloen-Korppi, E. Damskägg, J.-M. Pirkkalainen, M. Asjad, A. A. Clerk, F. Massel, M. J. Woolley, and M. A. Sillanpää, Stabilized entanglement of massive mechanical oscillators, Nature (London) **556**, 478 (2018).
[45] R. Riedinger, A. Wallucks, I. Marinković, C. Löschnauer, M. Aspelmeyer, S. Hong, and S. Gröblacher, Remote quantum entanglement between two micromechanical oscillators, Nature (London) **556**, 473 (2018).

[46] F. Massel, S. U. Cho, J.-M. Pirkkalainen, P. J. Hakonen, T. T. Heikkilä, and M. A. Sillanpää, Multimode circuit optomechanics near the quantum limit, Nat. Commun. **3**, 987 (2012).

[47] D. E. McClelland, N. Mavalvala, Y. Chen, and R. Schnabel, Advanced interferometry, quantum optics and optomechanics in gravitational wave detectors, Laser Photonics Rev. **5**, 677 (2011).

[48] S. Qvarfort, A. Serafini, P. F. Barker, and S. Bose, Gravimetry through non-linear optomechanics, Nat. Commun. **9**, 3690 (2018).

[49] H. Yu, L. McCuller, M. Tse, N. Kijbunchoo, L. Barsotti, N. Mavalvala, and L. S. Collaboration, Quantum correlations between light and the kilogram-mass mirrors of LIGO, Nature (London) **583**, 43 (2020).

[50] K. Stannigel, P. Komar, S. J. M. Habraken, S. D. Bennett, M. D. Lukin, P. Zoller, and P. Rabl, Optomechanical Quantum Information Processing with Photons and Phonons, Phys. Rev. Lett. **109**, 013603 (2012).

[51] R. Horodecki, P. Horodecki, M. Horodecki, and K. Horodecki, Quantum entanglement, Rev. Mod. Phys. **81**, 865 (2009).

[52] H. J. Kimble, The quantum internet, Nature (London) **453**, 1023 (2008).

[53] Y. Ma, H. Miao, B. H. Pang, M. Evans, C. Zhao, J. Harms, R. Schnabel, and Y. Chen, Proposal for gravitational-wave detection beyond the standard quantum limit through EPR entanglement, Nat. Phys. **13**, 776 (2017).

[54] R. Fleury, D. Sounas, and A. Alù, An invisible acoustic sensor based on parity-time symmetry, Nat. Commun. **6**, 5905 (2015).

[55] T. Yang, X. Bai, D. Gao, L. Wu, B. Li, J. T. L. Thong, and C.-W. Qiu, Invisible sensors: Simultaneous sensing and camouflaging in multiphysical fields, Adv. Mater. **27**, 7752 (2015).

[56] G. B. Malykin, The Sagnac effect: Correct and incorrect explanations, Phys. Usp. **43**, 1229 (2000).

[57] S. Kim, J. M. Taylor, and G. Bahl, Dynamic suppression of Rayleigh backscattering in dielectric resonators, Optica **6**, 1016 (2019).

[58] C. W. Gardiner and P. Zoller, *Quantum Noise* (Springer, Berlin, 2000).

[59] E. X. DeJesus and C. Kaufman, Routh-Hurwitz criterion in the examination of eigenvalues of a system of nonlinear ordinary differential equations, Phys. Rev. A **35**, 5288 (1987).

[60] See the Supplemental Material at http://link.aps.org/supplemental/10.1103/PhysRevLett.125.143605 for more technical details of our system, which includes Refs. [61–67].

[61] R. Reimann, M. Doderer, E. Hebestreit, R. Diehl, M. Frimmer, D. Windey, F. Tebbenjohanns, and L. Novotny, GHz Rotation of an Optically Trapped Nanoparticle in Vacuum, Phys. Rev. Lett. **121**, 033602 (2018).

[62] J. Ahn, Z. Xu, J. Bang, Y.-H. Deng, T. M. Hoang, Q. Han, R.-M. Ma, and T. Li, Optically Levitated Nanodumbbell Torsion Balance and GHz Nanomechanical Rotor, Phys. Rev. Lett. **121**, 033603 (2018).

[63] Y. Bellouard, A. A. Said, and P. Bado, Integrating optics and micro-mechanics in a single substrate: A step toward monolithic integration in fused silica, Opt. Express **13**, 6635 (2005).

[64] J. Chen, G. Zhou, L. Zhang, and W. Sun, Influence of intermolecular force on the head-disk interface of HDD with high recording density, in *2009 Symposium on Photonics and Optoelectronics (IEEE, New York, 2009)*, pp. 1–4.

[65] L. Wu and D. B. Bogy, Effect of the intermolecular forces on the flying attitude of sub-5 NM flying height air bearing sliders in hard disk drives, J. Tribol. **124**, 562 (2002).

[66] R. J. Joyce, H. F. Sterling, and J. H. Alexander, Silicon oxide and nitride films deposited by an r.f. glow-discharge, Thin Solid Films **1**, 481 (1968).

[67] H. Sugiura, R. Ikeda, K. Kondo, and T. Yamadaya, Densified silica glass after shock compression, J. Appl. Phys. **81**, 1651 (1997).

[68] G. Adesso, A. Serafini, and F. Illuminati, Extremal entanglement and mixedness in continuous variable systems, Phys. Rev. A **70**, 022318 (2004).

[69] R. Simon, Peres-Horodecki Separability Criterion for Continuous Variable Systems, Phys. Rev. Lett. **84**, 2726 (2000).

[70] G. C. Righini, Y. Dumeige, P. Féron, M. Ferrari, G. N. Conti, D. Ristic, and S. Soria, Whispering gallery mode microresonators: Fundamentals and applications, Riv. Nuovo Cimento **34**, 435 (2011).

[71] H. Lü, Y. Jiang, Y.-Z. Wang, and H. Jing, Optomechanically induced transparency in a spinning resonator, Photonics Res. **5**, 367 (2017).

[72] P. Kurpiers, P. Magnard, T. Walter *et al.*, Deterministic quantum state transfer and remote entanglement using microwave photons, Nature (London) **558**, 264 (2018).

[73] A. A. Maznev, A. G. Every, and O. B. Wright, Reciprocity in reflection and transmission: What is a 'phonon diode'?, Wave Motion **50**, 776 (2013).

[74] J. Li, S.-Y. Zhu, and G. S. Agarwal, Magnon-Photon-Phonon Entanglement in Cavity Magnomechanics, Phys. Rev. Lett. **121**, 203601 (2018).

[75] L. DiCarlo, M. D. Reed, L. Sun, B. R. Johnson, J. M. Chow, J. M. Gambetta, L. Frunzio, S. M. Girvin, M. H. Devoret, and R. J. Schoelkopf, Preparation and measurement of three-qubit entanglement in a superconducting circuit, Nature (London) **467**, 574 (2010).

[76] W. Qin, A. Miranowicz, P.-B. Li, X.-Y. Lü, J. Q. You, and F. Nori, Exponentially Enhanced Light-Matter Interaction, Cooperativities, and Steady-State Entanglement Using Parametric Amplification, Phys. Rev. Lett. **120**, 093601 (2018).

[77] T. M. Karg, B. Gouraud, C. T. Ngai, G.-L. Schmid, K. Hammerer, and P. Treutlein, Light-mediated strong coupling between a mechanical oscillator and atomic spins 1 meter apart, Science **369**, 174 (2020).